Received: 20 May 2021 | Accepted: 12 July 2021

DOI: 10.1111/ppl.13515

UPTAKE, TRANSPORT AND ASSIMILATION

Physiologia Plantarum

Loss of LaMATE impairs isoflavonoid release from cluster roots of phosphorus-deficient white lupin

Yaping Zhou[1] | Philipp Olt[1] | Benjamin Neuhäuser[1] | Narges Moradtalab[1] | William Bautista[2] | Claudia Uhde-Stone[2] | Günter Neumann[1] | Uwe Ludewig[1]

[1]Institute of Crop Science, Nutritional Crop Physiology, University of Hohenheim, Stuttgart, Germany

[2]Department of Biological Sciences, California State University, Hayward, California, USA

Correspondence
Uwe Ludewig, Institute of Crop Science, Nutritional Crop Physiology, University of Hohenheim, Stuttgart D-70593, Germany.
Email: u.ludewig@uni-hohenheim.de

Funding information
China Scholarship Council; Deutsche Forschungsgemeinschaft

Edited by: J. Schjoerring

Abstract

White lupin (*Lupinus albus* L.) forms brush-like root structures called cluster roots under phosphorus-deficient conditions. Clusters secrete citrate and other organic compounds to mobilize sparingly soluble soil phosphates. In the context of aluminum toxicity tolerance mechanisms in other species, citrate is released via a subgroup of MATE/DTX proteins (multidrug and toxic compound extrusion/detoxification). White lupin contains 56 *MATE/DTX* genes. Many of these are closely related to gene orthologs with known substrates in other species. *LaMATE* is a marker gene for functional, mature clusters and is, together with its close homolog *LaMATE3*, a candidate for the citrate release. Both were highest expressed in mature clusters and when expressed in oocytes, induced inward-rectifying currents that were likely carried by endogenous channels. No citrate efflux was associated with LaMATE and LaMATE3 expression in oocytes. Furthermore, citrate secretion was largely unaffected in P-deficient composite mutant plants with genome-edited or *RNAi*-silenced *LaMATE* in roots. Moderately lower concentrations of citrate and malate in the root tissue and consequently less organic acid anion secretion and lower malate in the xylem sap were identified. Interestingly, however, less genistein was consistently found in mutant exudates, opening the possibility that LaMATE is involved in isoflavonoid release.

1 | INTRODUCTION

Phosphorus (P) is an essential macroelement required by plants, but this element has low phyto-availability in most soils (Raghothama, 1999; Vance et al., 2003). To increase the availability of soil P_i (inorganic phosphate, the chemical form in which P is taken up and used in metabolism), various plant species form so-called cluster roots as specialized brush-like structures that massively release organic acid anions to mobilize P_i and also organic P_o from metal-P_i complexes on soil surfaces via ligand exchange (Gardner et al., 1981; Gardner et al., 1983; Wang & Lambers, 2020; Wasaki et al., 1999). Cluster roots are particularly abundant in various indigenous plant species from Australia, South America, and South Africa that are adapted to very low soil P, mainly members of the Proteaceae (Purnell, 1960). The leguminous crop *Lupinus albus* (white lupin) also forms cluster roots under P deficiency and has served for decades as a model to uncover cluster root development and physiology (Lambers et al., 2015; Watt & Evans, 1999). Clusters not only increase the root surface area to enhance P_i acquisition, but the increased surface area together with metabolic alterations in mature clusters also mediate the exudation of large amounts of carbon metabolites comprising up to 23% of the fixed carbon (Neumann & Römheld, 2007). Citrate is the dominant organic acid anion released in pulses of 1–3 days from mature clusters of P-deficient white lupin roots (Neumann et al., 1999). Prior to this main peak of citrate excretion, malate and isoflavonoids, primarily genistein, hydroxygenistein, and its mono- and diglycosides, are also secreted in large amounts into the rhizosphere (Neumann et al., 1999; Weisskopf, Abou-Mansour, et al., 2006). The transporter responsible for the malate release was

This is an open access article under the terms of the Creative Commons Attribution License, which permits use, distribution and reproduction in any medium, provided the original work is properly cited.
© 2021 The Authors. *Physiologia Plantarum* published by John Wiley & Sons Ltd on behalf of Scandinavian Plant Physiology Society.

recently identified and is encoded by *LaALMT1* (Zhou et al., 2020). Isoflavonoids and their glycosides inhibit bacterial and fungal consumption of the released citrate (Weisskopf et al., 2005; Weisskopf, Tomasi, et al., 2006), attract beneficial rhizobacteria for root nodule symbiosis and also help solubilizing P_i from metal-P_i complexes by indirect redox and solubilization effects on the metal (Tomasi et al., 2008). Phosphatases, as well as protons, are also released into the rhizosphere, allowing soil phosphate mobilization via hydrolysis of organic P and subsequent P_i acquisition (Dinkelaker et al., 1989; Neumann & Martinoia, 2002; Neumann & Römheld, 1999).

Citrate is also massively released from white lupin cluster roots when exposed to aluminum (Al), to chelate this toxic metal externally and prevent it from damaging the root (Wang et al., 2007). Such an Al detoxification mechanism exists also in many other species and involves multidrug and toxin extrusion/detoxification (MATE/DTX) membrane proteins. These were initially identified in the monocots barley (Furukawa et al., 2007) and sorghum (Magalhaes et al., 2007). The rice MATE/DTX transporter OsFRDL1 also transports citrate, but in another physiological context: it is expressed in the root pericycle and is involved in Fe-citrate translocation into the xylem (Yokosho et al., 2009). FRD3, a citrate transporter from the dicot *Arabidopsis* is also localized in the vascular cylinder of roots and has a similar function (Durrett et al., 2007). Various MATE/DTX proteins with proven citrate transport function contain a "citrate exudation motif domain" of roughly 50 amino acids that is absent from MATE/DTX proteins with other substrate specificities (Upadhyay et al., 2019). Structurally more distinct *MATE/DTX* genes display functions in secondary metabolite transport (flavonoid, xenobiotic, and alkaloid), in phytohormone transport (abscisic acid and salicylic acid) or even have nonorganic substrates, such as chloride (Takanashi et al., 2014; Upadhyay et al., 2019). At least some MATE/DTXs transport flavonoids or flavonoid glycosides and the substrate transport is typically accomplished by antiport with H^+ (Marinova et al., 2007; Takanashi et al., 2014; Zhao et al., 2011; Zhao & Dixon, 2009).

Members of the large *MATE/DTX* gene family are candidates for metabolite efflux transporters in white lupin cluster roots. These include *LaMATE*, a gene that has been characterized previously because it is upregulated under P-deficient conditions and is strongly expressed in mature clusters (O'Rourke et al., 2013; Secco et al., 2014; Uhde-Stone et al., 2005; Wang, Straub, et al., 2014). However, this plasma membrane localized protein did not complement the *frd3* phenotype in Arabidopsis (Uhde-Stone et al., 2005). We analyzed the genomic *MATE/DTX* gene inventory of white lupin and hypothesized that LaMATE mediates efflux of citrate or other metabolites by a H^+ antiport mechanism from P-deficient cluster roots. We therefore functionally studied LaMATE and its close homolog LaMATE3 in *Xenopus* oocytes and characterized *mate* mutants.

2 | MATERIALS AND METHODS

2.1 | Alignment and phylogenetic analysis

MATE/DTX proteins from white lupin were collected using the www.whitelupin.fr database and homologs from *Arabidopsis* were collected from www.aramemnon.de. Each sequence was used to search with BLAST for all homologous sequences in both genomes. A number for each lupin MATE/DTX was given, when possible, according to its nearest homolog in Arabidopsis (Tables S2 & S3). As not all members had a direct ortholog, some numbers were given arbitrarily. Phylogenetic analysis used ClustalW and CLC sequence Viewer 7.

2.2 | *qPCR*, plasmid vector preparation

For quantitative *RT-PCR*, total RNA was extracted with the innuPREP Plant Extraction kit from Analytik Jena, DNA was removed by DNAse and the RNA concentration was measured using a NanoDrop2000 spectrophotometer (Thermo Fisher Scientific Inc., Waltham, MA). Reverse transcription was performed with QuantiTect Reverse Transcription Kit (Qiagen GmbH, Hilden) according to the manufacturers instructions. The *RT-PCR* was set up with GreenMasterMix (GENAXXON bioscience, Ulm) and a C1000 Thermo Cycler attached to a CFX 384 real-time system (Bio-Rad Laboratories Ltd., Watford). Each reaction volume of 15 µl contained 10 ng of cDNA. *PP2A* and *UBC* genes were used for referencing. Used primers for *LaMATE* (*Lalb_Chr25g0283071*, *LAGI01_21605*, *LAGI02_29515*) and *LaMATE3* (*Lalb_Chr25g0283091*, and *LAGI02_168*) are shown in Table S1.

The CRISPR vectors used are based on *pCas9-TPC* (Schiml et al., 2016) and were called *pCas9::MATEPS1* and *pCas9::MATEPS2* (*PS* for protospacer). These vectors contain a *bar* selection gene, a 20-nt target region (protospacer) and the 5′-NGG protospacer adjacent motif (PAM) for Cas9 cleavage.

2.3 | Electrophysiology and transport assays in *Xenopus* oocytes

The coding regions of *LaMATE* and *LaMATE3* were amplified from white lupin *cDNA* and subcloned into the oocyte expression vector pOO2 (Ludewig et al., 2002). Complementary RNA (cRNA) was prepared from the linearized (MluI) plasmid DNA template using the mMESSAGE mMACHINE® Kit (Life Technologies GmbH, Darmstadt, Germany) following the manufacturer's instructions. The cRNA was divided into 2 µl aliquots and stored at −80°C until injection. The electrophysiological methods were conducted according to Mayer & Ludewig, 2006. Briefly, oocytes were obtained from Ecocyte Bioscience (Castrop-Rauxel), presorted and injected with 50 nl either water, *LaMATE*, or *LaMATE3* cRNA and incubated in ND96 at 18°C for 3–4 days. Recordings were performed in both control oocytes, *LaMATE*- and *LaMATE3*-expressing oocytes that were preloaded or not with citrate or water 0.5–2 h prior to the recording. Preloading was achieved by injecting each cell with 50 nl of 30 mM potassium citrate (pH 7.2).

The ND 96 solution (mM) was composed of 96 NaCl, 2 KCl, 1 $MgCl_2$, 1.8 $CaCl_2$, 2.5 Na-pyruvate, 5 HEPES, pH adjusted to 7.4 with NaOH. The recording solution (mM) was 110 choline chloride, 2 $CaCl_2$, 2 $MgCl_2$, and 5 MES, pH adjusted to pH 5.0 or pH 7.4 with Tris. The oocytes were clamped in most experiments to −30 mV (in some

experiments to 0 mV) and the currents were measured after stepping from this holding potential to different test potentials in−20 mV steps (+40 mV to −160 mV) for periods of 380 ms. For the current–voltage plots, the current at each voltage at the ultimate 50 ms (at which the currents reached a steady state) was averaged and plotted against the voltage. The I–V plots were the averaged data of different batches, the traces are examples of individual, representative oocytes.

For determination of citrate efflux, 50 nl of 30 mM ^{13}C-labeled citrate (Sigma Aldrich, pH 7.2) were injected into oocytes expressing LaMATE or LaMATE3. Citrate flux assays were performed in ND96 at pH 5.0. The oocytes were washed three times with washing solution and then three oocytes each were transferred into 300 µl fresh recording solution for 3 h incubation at 20°C. Subsequently, the oocytes were washed again twice. Then the groups of three oocytes were transferred into prebalanced tin cups and stored at 20°C. The external buffer and freeze-dried oocytes were dried and subjected to measurement of total ^{13}C abundance by isotope mass spectrometry (Delta Plus Advantage, Thermo Fisher Scientific), coupled to an Eurovector EA 3000 elemental analyzer.

The LaMATE-mediated genistein transport in oocytes was evaluated in the following manner: For efflux, 50 nl of 10 mM genistein (dissolved in 40% [v/v] DMSO, Roche) were preloaded into 3- day-incubated oocytes preinjected with *LaMATE* cRNA. The oocytes were allowed to recover and reseal for several minutes. Then oocxtes were washed three times with ND96 solution. Pairs of visually inspected healthy looking oocytes were placed into 100 µl choline chloride solution. After 120 min of incubation, 75 µl of the incubation solution were removed, freeze-dried and dissolved in 75 µl methanol for the measurement. For uptake, 3- day-expressing oocytes were placed in ND96 solution containing 10 mM genistein (predissolved in DMSO:ND96 40%:60% [v/v], pH 7.4) for 4 h. The uptake was terminated by washing twice in ND96 solution and once with MQ water. Oocytes were then visually inspected and only healthy oocytes were separated in groups of three into Eppendorf tubes. The genistein was extracted by mechanical disruption of the oocytes. Eighty-five micro liter methanol were added, the solution was thoroughly mixed and centrifuged for 2 min at 18 000*g*. Seventy-five micro liter of the supernatant were harvested and analyzed by mass spectrometry. In- and efflux experiments were replicated once with similar results.

2.4 | *Agrobacterium rhizogenes*-mediated lupin transformation for genome editing

Agrobacterium rhizogenes strain A4T (Quandt et al., 1993) was employed for hairy root transformation. Plasmids were transfected into this strain, positive colonies were selected and subsequently cultured in LB liquid medium with 100 µM spectinomycin and 50 µM rifampicin until the OD_{600} reached 0.8. Cells were centrifuged and resuspended in Murashige and Skoog medium (Duchefa) containing 20 µM acetosyringone for explants inoculation.

White lupin seeds (*L. albus* cv Orus) were surface sterilized in 70% (v/v) ethanol for 20 min followed by 12% (v/v) commercial bleach ($NaClO_3$) containing two drops of tween-20 for 6 min and five washes with sterile deionized water. Seeds were plated on wet filter paper and germinated overnight in darkness at 23°C. From germinated seeds with approximately 10 mm radicles, approximately 3 mm tip sections were removed with a sterile scalpel. The radicles were inoculated with the appropriated *A. rhizogenes* containing either the *LaMATEPS* constructs or empty vector (EV) control constructs, and co-cultivated on Murashige and Skoog plates containing 150 µM acetosyringone for three days (Zhou et al., 2019).

Six seedlings were placed on 75 ml slanted agarose (0.6% in 1× Hoagland solution; Uhde-Stone et al., 2005) in transparent round trays with covers. Plates were then vertically placed in an incubator at 25°C with 16 h photoperiod and a light intensity of about 200 µmol s^{-1} m^{-2}. Seedlings were transferred into P-deficient hydroponics after two week incubation. For the Al treatment, precultured P-deficient plants were treated for 2 days in 2.5 mM $CaCl_2$ solution containing 20 µM $AlCl_3$ at pH 4.5 before final harvest (Zhou et al., 2020).

2.5 | *RNAi*-based silencing of the *LaMATE* gene

LaMATE silencing in white lupin roots (genotype Amiga) by *RNAi* was performed as described previously (Uhde-Stone et al., 2005). In brief, a 500-bp PCR fragment containing the 5′ coding region of *LaMATE* was inserted into *pHellsgate8* to generate an *hpRNA* expression construct for *RNAi*-based gene silencing (Helliwell & Waterhouse, 2003). Lupin roots were transformed via *A. rhizogenes* with this *LaMATE RNAi* construct and with the empty-vector control, respectively. Kanamycin (15 mg l^{-1}) was used for selection of transgenic roots; mutants and EV control plants were grown under −P conditions to induce *LaMATE* expression, and were then tested for organic acid excretion.

2.6 | Mutation (indel) screen assay and genotyping

Genomic DNA from white lupin transgenic roots was extracted using quick genomic DNA extraction method (Edwards et al., 1991) and the genomic regions containing the target sites were amplified. The protocol for PCR reactions was set as: an initial denaturation of 98°C for 2 min, 30 cycles of 98°C 30 s, 55°C 30 s, 72°C 2 min, and an extension of 72°C for 10 min. PCR products of *MATEPS1* plants, purified from agarose gel, were digested with 0.5 µl HindIII for 1 h at 37°C and then subjected to 1.5% agarose gel electrophoresis. For genotyping of *matePS1* and *matePS2* mutant roots, PCR products covering the protospacer site were amplified with specific primers (Table S1) and were subjected to sequencing. Multi-sequence alignment was conducted to screen for indels.

2.7 | Root exudate, root tissue, xylem sap sampling, and analysis

The whole root system of plants grown in hydroponics was rinsed three times with water before it was submerged in aerated deionized

water for 2 h for exudate collection, and 10 ml subsamples of the exudates solution were membrane filtered through 0.2 μm pore size and frozen at–20°C until analysis. For xylem sap collection, shoot parts were removed with a sterilized razor; the cut was cleaned with a paper towel to remove cell debris, and sorption filter papers were placed on the wounded surface. As the phloem is quickly closed by the wounded plant, sap collected for 2 h mainly represents xylem sap. The volume of the collected sap was gravimetrically quantified to account for potentially different flow rates. The xylem sap was extracted with 200 μl distilled water and frozen at −20°C.

The subsamples were analyzed for organic acid concentrations and phenolics by reversed-phase high performance liquid chromatography (HPLC), as previously described (Haase et al., 2007; Neumann et al., 1999). Briefly, the separation of organic acids was conducted on a reversed phase column (250 mm long, 4 mm i.d.; GROM-SIL 120 ODS-3CP, 5 μm particle size) equipped with guard column (20 mm long, 4 mm i.d.) with the same stationary phase (Dr. Maisch HPLC GmbH). Sample solutions (20 μl) were injected onto the column, and 18 mM KH_2PO_4 (adjusted to pH 2.1 with H_3PO_4) was used for isocratic elution with a flow rate of 0.7 ml min^{-1} at 40°C and UV detection at 210 nm. Identification of organic acids was performed by comparing retention times and absorption spectra with those of known standards. The identity of the major organic acids malic acid and citric acid was additionally confirmed by enzymatic analysis with organic acid test kits (RBiopharm AG).

For the *LaMATE RNAi* plants, five plants and five empty-vector control plants were grown for 6 weeks in −P conditions. Roots were then placed into 25 ml aerated H_2O. After 1 h, the bathing medium was sterile-filtered, concentrated via speedvac and purified by anion exchange chromatography. Organic acids were then separated by HPLC (SP800 pump and Sp4290 integrator; Spectra-Physics) equipped with an Aminex HPX-87H, 300-X 7.8 mm column (Bio-Rad) and an organic acid guard column (Bio-Rad). Then, 0.008 N H_2SO_4 was used as eluent with a flow rate of 0.6 ml min^{-1} at room temperature. Organic acids were detected at 210 nm on a Spectroflow 757 UV/VIS detector (ABI Analytical Kratos Division) and compared to an organic acid standard consisting of oxalate, citrate, malate, succinate, formate, and acetate.

For the determination of phenolics, the mobile phase consisted of phosphate buffer (18 mM KH_2PO_4, pH 2.1 adjusted with H_3PO_4) and methanol. Samples were eluted with the following linear gradients: from 0 to 15 min 40% methanol (60% phosphate buffer) to 100% methanol, then 5 min 100% methanol and from 20 to 25 min 100% methanol to 60% phosphate buffer to re-establish the initial conditions before the injection of another sample. The flow rate was 1 ml min^{-1}, the injection volume was 20 μl and column temperature was maintained at 40°C. The gradient elution was performed on a reversed phase C-18 column (GROM-SIL 120 ODS ST, 5 μm particle size, 290 * 4.6 mm), equipped with a 20 * 4.6 mm guard column with the same stationary phase (Dr. Maisch HPLC GmbH), with direct UV detection at 270 nm. Genistein identification was performed by comparison of retention times and absorption spectra with a genistein standard (ROTH) and by HPLC-MS analysis on a Waters ACQUITY CSH C18, 1.7 μm, 2.1 × 150 mm column (Waters Corp. Milford) with a flow rate of 0.3 ml min^{-1}, temperature 40°C and an injection volume of 5 μl. The separation by HPLC-MS was conducted by a formic acid/acetonitrile gradient and quantification was conducted by comparison with an external genistein standard. The same analysis pipeline was used for genistein efflux experiments in oocytes.

2.8 | Shoot metal element determination

Shoots of control and hairy root transformed lupin were oven-dried at 55°C for 5 days, milled and 200 mg of dried shoot material was ashed for 5 h in a muffle furnace at 500°C. After cooling, the samples were extracted twice with 1 ml of 3.4 M HNO_3 and evaporated until dryness to precipitate SiO_2. The ash was dissolved in 1 ml of 4 M HCl, subsequently diluted 10-fold with hot deionized water, and boiled for 2 min. Fe, Mn, Zn, and Cu concentrations were measured using atomic absorption spectrometry (ATI Unicam Solaar 939, Thermo Electron). Potassium (K) and calcium (Ca) were measured by flame emission photometry (ELEX 6361, Eppendorf).

2.9 | Statistical analysis

The data were analyzed by ANOVA with least significant difference test using the SAS for windows Version 9.4 (SAS Institute Inc., USA) and by ANOVA with Tukey's post hoc-test using R version 3.6.0 (R Development Core Team, 2008) and the multcomp package (v1.4-12; Hothorn et al., 2008). Statistically significant differences (P <0.05) are indicated with different letters in the figures.

2.10 | Accession numbers

LaMATE (*Lalb_Chr25g0283071*) and *LaMATE3* (*Lalb_Chr25g0283091*).

3 | RESULTS

3.1 | The complete gene family encoding MATE transporters in *L. albus*

The genome of white lupin (Hufnagel et al., 2020; Xu et al., 2020) contains 56 *MATE/DTX* gene family members (Table S2), a similar number as the 57 *MATE/DTX* genes in Arabidopsis (Table S3, Figure 1). The hydrophobic proteins predicted from the gene sequences contain between 400 and 571 amino acids. All have a similar topology, which matches that of various crystallized eukaryotic MATE/DTX proteins. These typically have an intramolecular pseudo-twofold symmetry with 12 helical transmembrane spans. This suggests that this protein architecture is conserved in all white lupin MATE/DTXs. In Arabidopsis,

only two MATE/DTX proteins contain a *bona-fide* "citrate exudation motif domain" (Upadhyay et al., 2019), but within the white lupin genome, we identified eight MATE members with this motif (Figure 1A). Of these, the transcripts of only four members had been detected in functional cluster roots in our previous analyses, with *LaMATE* and *LaMATE3* expressed at the highest level in mature clusters (Figure 1A, Wang, Straub, et al., 2014). Within this group of citrate transporter-related MATEs, there is a gene triplication (*LaMATE*, *LaMATE2*, and *LaMATE3*) with three similar genes adjacent to each other on chromosome 25.

By contrast, most white lupin MATE/DTXs members have one close homolog on a different chromosome. This is in agreement with the recent genome duplication in this species, but unique sequences were also identified. For building a phylogenetic tree of all white lupin MATE/DTXs, we included several members with functionally proven substrates, mostly from Arabidopsis (Figure 1B, Table S3). These include AtDTX14, which has been crystallized and exports the antibiotic norfloxacin (Miyauchi et al., 2017), the vacuolar flavonoid/H^+-antiporter AtTT12 (Marinova et al., 2007), the putative flavonoid transporter AtDTX35 (Kitamura et al., 2016), which also mediates chloride currents (Zhang et al., 2017), the abscisic acid efflux carrier AtDTX50 (Zhang et al., 2014), the salicylic acid transporter AtDTX47 (Serrano et al., 2013), and AtMATE and AtFRD3, which both contain the "citrate transporter motif" and apparently transport citrate (Durrett et al., 2007; Liu et al., 2009). Interestingly, members of MATE transporters with "citrate motif" represent (together with salicylic acid-related MATE/DTXs and two other members) a group that is separated from most other MATE/DTXs (Figure 1B). Relatives of the

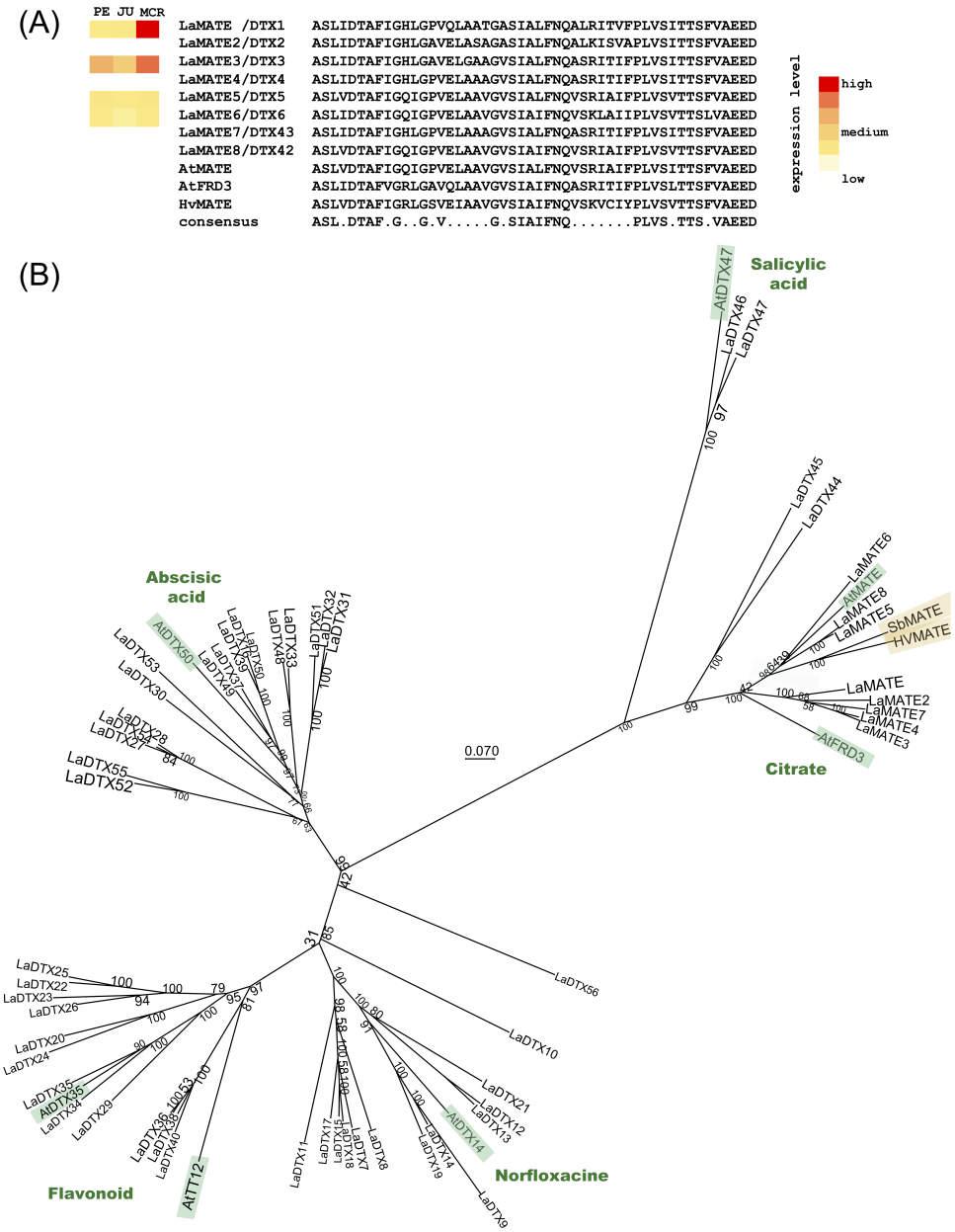

FIGURE 1 The inventory of *Lupinus albus* MATE/DTX proteins. (A) The "citrate transporter motif" of eight white lupin MATE/DTX members and their expression levels in pre-emergence (PE), juvenile (JU), and mature cluster roots (MCR) (data from Wang, Straub, et al., 2014); red: high, yellow: intermediate, white: low/not expressed. The same region in three functional citrate transporters from Arabidopsis and barley is also aligned. This region covers the end of the first transmembrane helix, the following loop and the entire second transmembrane span. (B) Phylogenetic relationships between all white lupin MATE/DTX proteins and functionally characterized MATE/DTXs from Arabidopsis (At; labeled green), barley (Hv; *Hordeum vulgare*, *yellow*) and *Sorghum bicolor* (Sb, yellow). Numbers represent bootstrap values obtained from 1000 trials. Transported substrates of the Arabidopsis homologs are given close to the individual transporters

abscisic acid transporting AtDTX50 are identified in a distinct sub-branch with 16 members and another sub-branch contains flavonoid and chloride-transporting AtMATE/DTXs. The crystallized norfoxacine-transporter AtDTX14 grouped with another sub-branch of white lupin MATE/DTXs (Figure 1B). Overall, the sequence similarity within these sub-groups strongly associates certain white lupin proteins with MATE/DTX orthologs that have known substrates (-Table S3); this analysis strongly predicts that LaMATE and LaMATE3 are citrate transporters.

We first used *qRT-PCR* to confirm the expression pattern of *LaMATE*. Expression was high in mature, functional, P-deficient clusters, but absent in nonfunctional, young or senescent clusters. The *LaMATE* transcript was also not detected in roots that received sufficient P and not in the leaves (Figure 2A). As citrate secretion steeply increases in mature clusters (Neumann et al., 1999), *LaMATE* matched the expected expression profile of a citrate release channel (or citrate release transporter). *LaMATE3* was also root-specific and highest expressed in mature clusters, but its expression was lower than that of *LaMATE* and it was also detected in other parts of the root, including P-sufficient lateral roots (Figure 2). These two transporter genes were chosen for further functional analysis.

3.2 | Expression of LaMATE and LaMATE3 in oocytes

We decided to examine the electrophysiological properties of LaMATE and LaMATE3 in the heterologous expression system *Xenopus laevis* oocytes by two-electrode voltage-clamp. As citrate is an anion and MATE/DTX transporters typically function as H^+-antiporters, we expected to record pH- and citrate-dependent currents, especially from oocytes preloaded with citrate. Previous

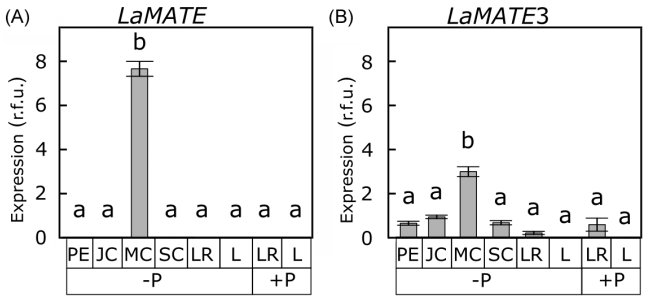

FIGURE 2 Expression of *LaMATE* and *LaMATE3* in roots at different developmental stages. (A) *LaMATE* and (B) *LaMATE3*. PE: pre-emergent cluster roots; JC: juvenile cluster roots, MC: mature cluster roots; SC: senescent cluster roots; LR: lateral roots without clusters; L: leaves; −P: treatment without phosphorus supply; +P: treatment with phosphorus supply in hydroponic solution; r.f.u.: relative fluorescence units; Different letters indicate significant differences at $P < 0.05$

electrophysiological analysis had pointed to the involvement of anion channels in the organic acid anion release in P-deficient white lupin roots (Zhang et al., 2004). We do not want to make a clear mechanistic distinction between citrate transporters or channels here and collectively use the term citrate transporters (which includes citrate channels).

Oocytes expressing LaMATE or LaMATE3 showed inward currents at membrane potentials more negative than −100 mV in six independent batches of oocytes (Figure 3A,C,D) that were not observed in water-injected control oocytes. However, there was only little current increase between −100 and +40 mV by LaMATE, and no increase by LaMATE3, compared to water-injected controls (Figure 3). These slowly activating inward currents were consistently larger in *LaMATE*- compared to *LaMATE3*-expressing oocytes and were bigger at pH 5.0 (which represents the apoplastic pH of functional clusters) than at pH 7.4 (Figure 3A,C,D). In the experiments shown in Figure 3A, oocytes were incubated in a recording solution with choline chloride, but the replacement with a ND96, a solution that mainly contains sodium as the monovalent cation, did not change the current characteristics, the amplitude was similar ($n = 3$). This excluded that choline was specifically related to the inward current. As the bulky cation choline does not permeate through typical (endogenous) cation channels, it was chosen in the recording solutions for further analysis. A potential charge carrier of the MATE- and MATE3-induced currents was therefore chloride, which was the dominant anion in the recording solutions. The reduction of the external chloride to 30 mM did only marginally change the MATE/MATE3-induced inward current amplitudes at highly negative voltages, but shifted the reversal potential by 18 ± 4 mV (LaMATE, $n = 3$) and 17 + 3 mV (LaMATE3, $n = 3$) toward more positive voltages, respectively, which is in line with chloride as the main charge carrier of these currents (in the absence of citrate).

We then evaluated whether citrate injection prior to recording (as 30 mM K-citrate, which is estimated to lead to ~3 mM internal citrate concentration) affected ionic currents in control (water-injected) oocytes. We found no increase of ionic currents between +40 and −160 mV by citrate injection (Figure 3A,B). To test whether LaMATE- or LaMATE3-expressing oocytes released citrate from the cells, a subset of oocytes was then also preinjected with potassium citrate before the recording. The currents by LaMATE3 at negative membrane potentials tended to be slightly reduced by citrate injection prior to the recording, but currents were similar in oocytes that expressed LaMATE, irrespective of preloading with citrate (except for the data point at −160 mV, where currents were [on average] slightly larger with citrate; Figure 3A,C,D, $n = 9$).

At pH 5, the reversal potential of endogenous ion currents (the voltage at which no outward or inward current was recorded) of water-injected controls was around −58 ± 9 mV (pH 5, $n = 12$) and was little affected by citrate injection −57 ± 8 mV (pH 5, $n = 7$). In *LaMATE*-expressing oocytes, the reversal was −37 ± 6 mV ($n = 8$) and

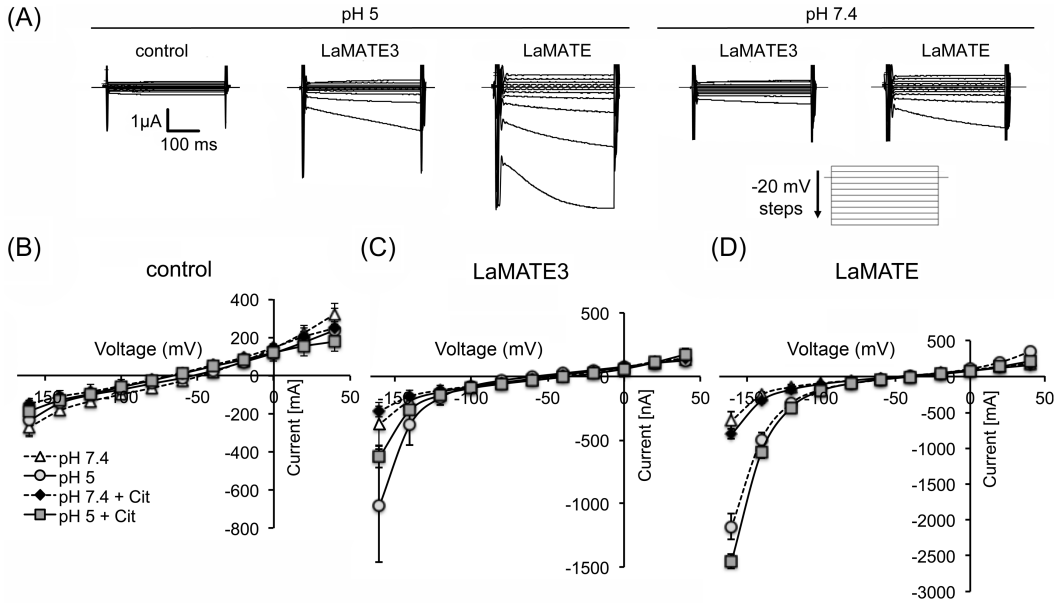

FIGURE 3 Functional characteristics of LaMATE3 and LaMATE expressed in *Xenopus* oocytes. (A) Representative current traces of control, *LaMATE3*- and *LaMATE*-expressing oocytes, elicited with voltage protocol in the inset, staring at 40 mV in −20 mV steps to −160 mV. Scaling bars: 1 μA (*y*-axis) and 100 ms (*x*-axis). Left traces in pH 5.0; right traces at pH 7.4. (B–D) Current–voltage relationships of noninjected (B), *LaMATE3*-expressing (C), and *LaMATE*-expressing (D) oocytes bathed in choline-based solution at pH 5.0 (circles and squares) and pH 7.4 (triangles and rhombs). Data points from oocytes preinjected with 50 nl of 30 mM K-citrate (rhombs, squares). Values represent the mean ± SE (n = 4–10) from one oocyte batch. Note the different y-axis scales in B, C, and D. Similar currents were recorded in a total of 6 oocyte batches, but the maximal current amplitude varied between the oocyte batches

with injected citrate −35 mV ± 4 mV (n = 12), respectively. The reversal of citrate-loaded oocytes expressing *LaMATE3* was similar, −35 ± 4 mV (n = 14), which is close to the reversal potential for chloride (at ~ −30 mV). At pH 7.4, the reversal potential of controls (n = 9), *LaMATE*- (n = 8), or *LaMATE3*-expressing (n = 7) oocytes was ~5 mV more negative, but also largely invariant to citrate injection ($n_{contr} = 8$, $n_{MATE} = 11$, $n_{MATE3} = 13$). These combined data strongly argue against substantial citrate transport in *LaMATE*- and *LaMATE3*-expressing oocytes (Figure 3C,D). Although the reversal potential for cotransporters is difficult to predict, a H+ symport mechanism was expected to shift the reversal to more positive values at more acidic pH, which was not observed and argues against substantial H^+ (co-)transport in oocytes expressing LaMATE and LaMATE3.

Although the ionic currents induced by LaMATE and LaMATE3 were little affected by internal citrate, we considered the possibility that citric acid release from preloaded oocytes might occur without net charge movement, which would then be nonelectrogenic and this might escape detection by ion current recordings. We therefore measured the release of ^{13}C-labeled citrate from oocytes expressing these proteins. In addition, we quantified the retention of label in the cells after 3 h incubation. Overall, no differences between oocytes expressing LaMATE, LaMATE3 and nonexpressing controls were found (Figure 4). Therefore, despite the evoked ionic currents in oocytes, no major citrate efflux activity was associated with *LaMATE*- and *LaMATE3*-expression in oocytes under the tested conditions (Figures 3 and 4).

3.3 | Composite lupin transgenics with mutated *LaMATE* in roots

To directly address LaMATE function in plant roots, we used a CRISPR/Cas9-mediated reverse genetic approach. We focused on *LaMATE* as the most specific and strongest expressed *MATE/DTX* gene in cluster roots that provoked large ionic currents in oocytes. To suppress *LaMATE* expression in roots, two independent CRISPR/Cas9 vectors were constructed. These targeted the gene at two independent sites. The target site for the first construct contained a HindIII restriction site for later mutant identification, which facilitated the estimation of the mutation efficiency. Simultaneous co-targeting of other *MATE* genes was unlikely, because of mismatches in the core sequences of other potential target sites. The extent of mutations and the variability of the mutations in the *LaMATE* sequence are shown for 16 *matePS1* transgenic composite white lupin plants (Figure 5A). Each transgenic root was randomly divided into three segments, indicated as #A, #B, and #C. Restriction analysis indicated that DNA fragments derived from the mutants were mostly resistant to digestion, indicating that mutations close to the protospacer adjacent motif (PAM) occurred, but residual cut fragments (and thus nonmutated genomic sequences close to the PAM) were also sometimes identified, indicating heterogeneity of genomic DNA in the sample (Figure 5A). Fragments were subsequently sequenced by Sanger methods and identified two deletion types, of 1 bp in #7A and #11B, and 27 bp in #4C (Figure 5B). Base pair exchanges ranging from 1 bp in #8A, #9B,

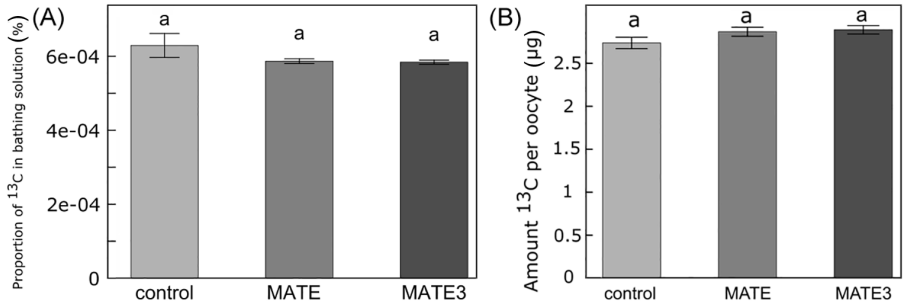

FIGURE 4 Lack of ^{13}C-labeled citrate efflux from LaMATE- and LaMATE3-expressing *Xenopus* oocytes. (A) Released and (B) retained ^{13}C-isotope in water-injected controls, *LaMATE*- and *LaMATE3*-expressing oocytes bathed in ND96 solution at pH 5.0. Values represent the mean ± SE (n = 6–11). This experiment was repeated with injected and well-expressing oocytes from an independent batch, which revealed the same result

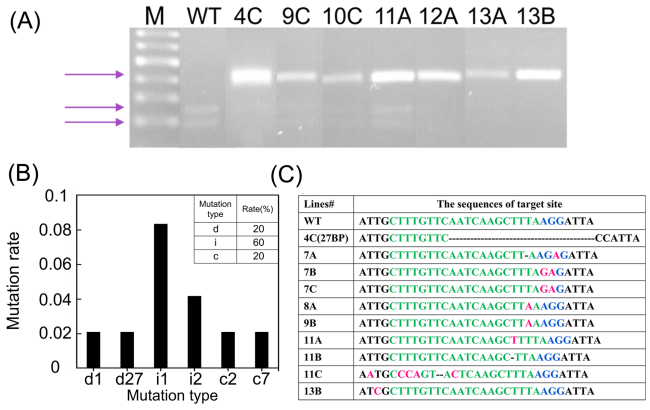

FIGURE 5 Mutation identification in CRISPR-targeted transgenic roots. (A) Detection of target mutations in composite plants generated by *A. rhizogenes* transformation by impaired *HindIII* restriction enzyme digestion. A 391 bp region surrounding the target by PCR from genomic DNA was amplified. EV: empty vector; wild-type, 4C-13B represent independent transgenic plants of sgRNA1-MATE (*matePS1*). Arrows indicate the digested and nondigested fractions. (B) The frequency of deletion (d), insertion/exchange (i) and combined (c) mutations. *x*-axis: d#, number of bases deletion at target site; i#, number of bases insertion at target site; c#, combined mutations. (C) Alignment of sequences with Cas9-induced mutations in the target sites of *LaMATE* gene. The wild-type sequence is shown at the top. The sequences targeted by the synthetic sgRNAs are shown in green, and mutations are shown in red

and #11A to 2 bp in #7B and #7C were also found around the expected cleavage site (Figure 5C). Combinations of these indicated that mixtures of mutations (deletions and exchanges/insertions) occurred in the target regions of individual plants (Figure 5C). These mutation types were randomly spread in the target region. Combined mutations occurred most frequently, up to 60%, followed by the insertion type (20%) and the deletion type (20%). Most of the mutations induced by the CRISPR/Cas9 system resulted in short nucleotide changes (≤ 3 bp), except in samples #4C and #13B. The mutations generally occurred close to the cleavage site, consistent with the results of previous CRISPR reports on soybean and rice (Li et al., 2015; Mikami et al., 2015).

3.4 | Citrate released from roots, in root tissue and in xylem sap

Composite transgenics with transgenic, *mate* mutant roots were grown hydroponically in −P conditions to quantify the citrate secretion from roots. Plants that underwent the same transformation protocol, but with EVs, were considered as wild-type in the *LaMATE* locus and served as controls. Mutant roots in individual sites were collected irrespective of the type of mutation that occurred at individual sites (*matePS1* and *matePS2*) and were handled as uniform mutants, although not all may represent full *loss-of-function* mutants. Compared to the controls, lower levels of citrate (Figure 6A) were found in exudates from plants targeted at the *matePS2* site (P <0.05). A similar trend was observed in the *matePS1* mutants. In P-deficient plants that were subsequently exposed to Al stress for two additional days, the citrate release was not significantly different from controls in both mutant groups (Figure 6B). However, total citrate release was not particularly stimulated after the 2 day Al supply; either the relatively high Al damaged the roots or they were already exhausted at the time of measurement. Interestingly, the moderate decrease of citrate in exudates under P-deficiency of *matePS2* mutants was paralleled by significantly diminished concentrations of citrate in the mutant root tissue (Figure 6C), which could explain the lower amount of released citrate. Because we could not exclude that there was residual functional LaMATE in these mutants, we investigated citrate exudation also in an independent approach where the *LaMATE* expression was reduced by silencing through *RNAi* (Uhde-Stone et al., 2005). The citrate exudation was, however, also consistently unaffected compared to the EV controls, confirming that citrate efflux remained, despite knockout or repression of *LaMATE* (Figure 6D).

Because the reduction of functional *LaMATE* apparently had an effect on citrate tissue concentrations, we considered the possibility that an overall change in the root carboxylate metabolism had occurred. We therefore also measured the internal concentrations of malate in the roots and in its exudate. Interestingly, we found a decrease of malate in *matePS2* mutant exudates by about 50%, which was paralleled by about 50% lower malate concentrations in P-deficient root tissue in these mutants (Figure 7A,B). A smaller, nonsignificant reduction compared to the EV control was seen for *matePS1*

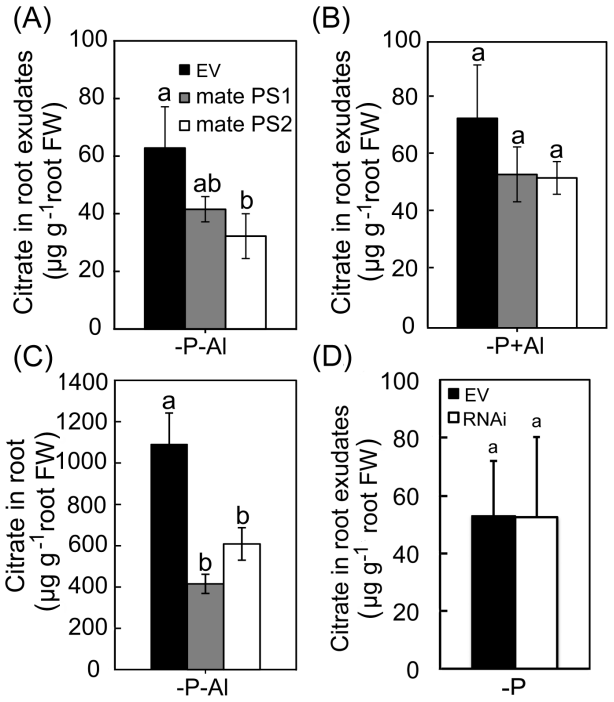

FIGURE 6 Citrate in root exudates and roots from control and mutant plants. (A) Citrate in root exudates of P-deficient composite transgenic CRISPR plants and (B) plants additionally exposed to Al for 2 days. Empty plasmid-transfected transgenics that were wild-type in the *LaMATE* locus served as controls (EV, black bars). Mutants for each target site (*matePS1*, gray bars and *mate PS2*, white bars) were grouped irrespective of the mutation that occurred in the individual root (which may not lead to complete *loss of function* of *LaMATE*; n = 8–12). (C) Citrate in the root tissue. (D) Citrate in root exudates of P-deficient composite transgenic *RNAi* plants (n = 5). Different letters indicate significant differences by one-way ANOVA (P <0.05)

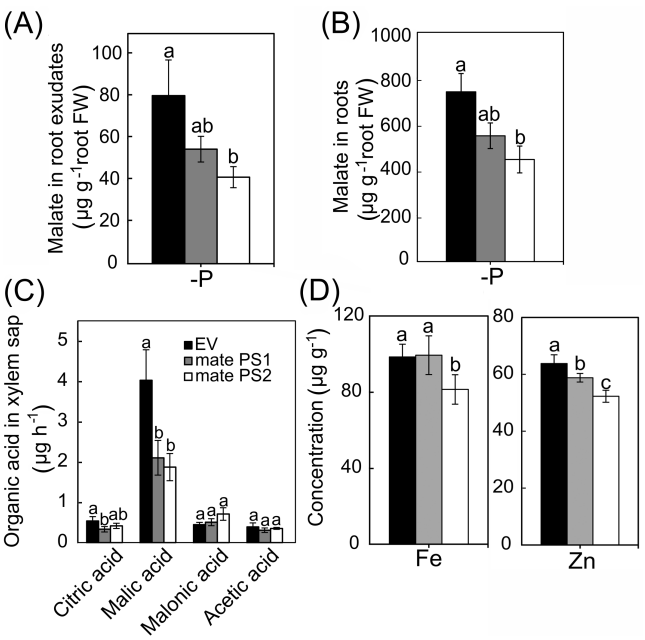

FIGURE 7 Malate in roots and root exudates from controls and mutants under P-deficiency. (A) Malate in root exudates of composite transgenic plants. (B) Malate in roots. (C) Organic acids in the xylem. (D) Iron and Zn in the shoot of P-deficient plants. Empty plasmid-transfected transgenics that were wild-type in the *LaMATE* locus served as controls (EV, black bars), mutants for each target site (*matePS1*, gray bars and *matePS2*, white bars). Different letters indicate significant differences by one-way ANOVA (P <0.05; n = 8–12)

(Figure 7A,B), suggesting that overall carboxylate metabolism was affected in the transgenics.

We hypothesized that the lower carboxylate levels in the roots might additionally result in lower carboxylate concentrations in the xylem sap and found that both *matePS* mutant groups consistently had only about half the concentration of carboxylates, mainly malate, in the xylem sap (Figure 7C). The concentration of citrate, which was always much lower than that of malate, was only significantly lowered in one *matePS* group compared to the controls (P < 0.05). Other carboxylates, such as acetate, malonate, trans-aconitate, and maleate, were also identified in the xylem sap, but at lower levels. These were indistinguishable between controls and transgenic roots (Figure 7C).

Since homologs of LaMATE in other species and the malate transporter LaALMT1 of white lupin (Zhou et al., 2020) participate in long distance metal-chelate translocation to the shoot, we determined the shoot concentrations of iron (Fe), zinc (Zn), copper (Cu), manganese (Mn), potassium (K), and calcium (Ca) under P-deficient conditions. Interestingly, compared with the control plants, the shoot concentration of Fe was slightly lower in the plants targeted with the *matePS2* construct. Zn was slightly lower in in both *matePS* mutant groups, which parallels the lower organic acids in the root tissue and in exudates (Figures 6 and 7). The concentration of other elements was unchanged in the transgenics.

3.5 | Isoflavonoid determination in root exudates

Although our phylogenetic analysis clearly positioned LaMATE within the "citrate motif" transporter group of MATE/DTXs, we ultimately considered the possibility that LaMATE was involved in the efflux of other compounds, such as isoflavonoids or their glycosides. These compounds are also exclusively released from mature clusters, but this release temporally just precedes the major peak of citrate exudation. Therefore, we measured HPLC profiles of root exudates from P-deficient control and mutant plants, using a methanol gradient. We identified several peaks in the HPLC chromatograms from root exudates, both from wild-type roots and *matePS* mutants. Surprisingly, one of these was specifically and consistently lower in *matePS* mutants, while others were somewhat variable, but not consistently different between genotypes (Figure 8A, n = 12). Interestingly, the elution time of this substance overlapped with that of purified genistein (Figure 8B). In both *matePS* mutant groups, the amount of this compound in root exudates was at least three-fold lower than in controls (Figure 8C, P <0.05). We ultimately purified the substance

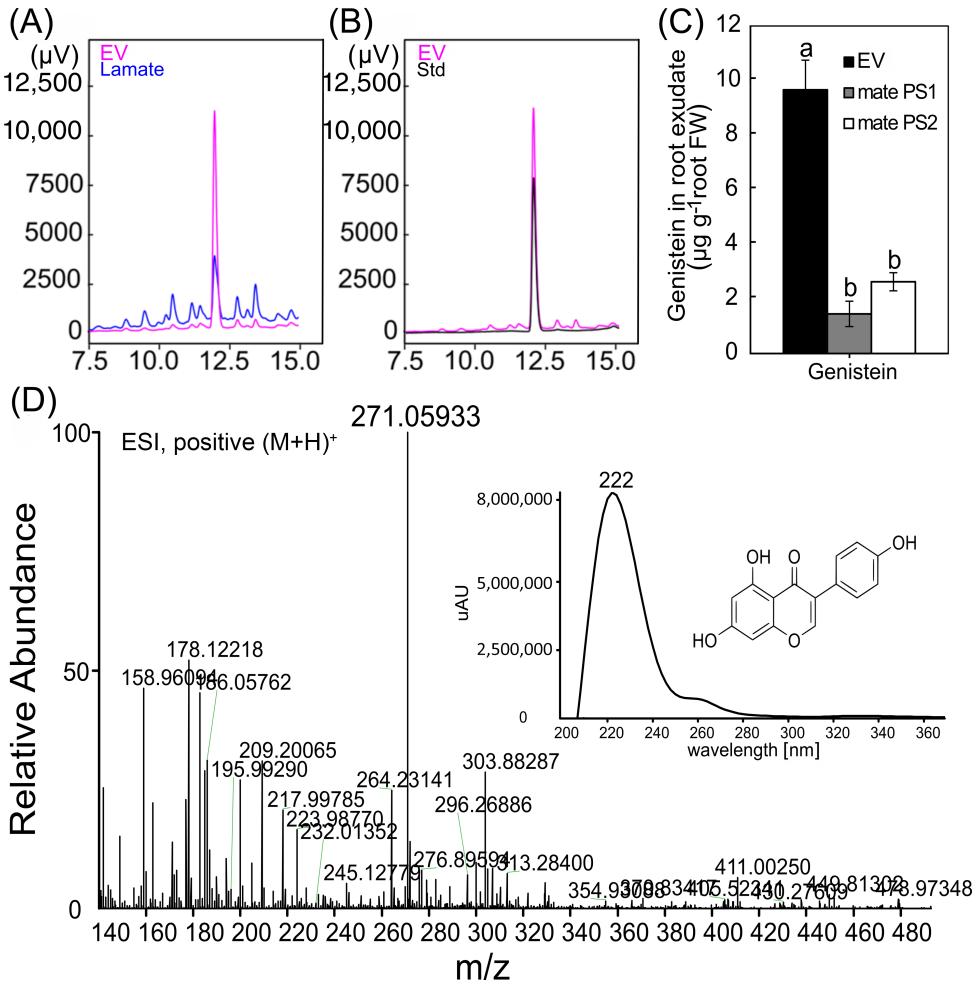

FIGURE 8 Identification of genistein as major decreased metabolite in exudates collected from mutants. (A) HPLC chromatograms obtained via methanol gradient from controls (red) and mutant (blue) exudates. (B) Overlap between the major peak from controls (red) and genistein standard (black). (C) Comparison of genistein quantity in empty plasmid-transfected transgenics that were wild-type in the *LaMATE* locus that served as controls (EV, black bars) and mutants for each target site (*matePS1*, gray bars and *matePS2*, white bars). (D) Mass spectrometric detection of genistein as major component in the exudate mixture from the controls. Inset: UV-absorption of genistein standard and its structure. Different letters indicate significant differences by one-way ANOVA ($P < 0.05$; $n = 8–12$)

underlying the chromatogram peak from control exudates and verified its identity as the isoflavonoid genistein by mass spectrometry (HPLC-MS, Figure 8D). These results agree with substantially declined genistein efflux from *matePS* mutant roots under P-deficiency compared to the controls. LaMATE did not affect genistein efflux from preloaded oocytes, which may corroborate that LaMATE did not functionally express in that system (Figure S1).

4 | DISCUSSION

4.1 | The *MATE/DTX* inventory in white lupin

White lupin has been a very successful model to study efficient physiological and morphological plant adaptations to phosphate deficiency (Cheng et al., 2011), but the transporters responsible for the massive exudation of citrate and flavonoids are not yet known. We identified 56 *MATE/DTX* genes in white lupin, a similar number as the 57 *MATE* genes in Arabidopsis. One of their family characteristics is the frequent appearance in pairs of closely related genes, but there were also unique genes (Figure 1). Interestingly, these were grouped into certain sub-branches for which the substrates of certain Arabidopsis orthologs are established. Although sequence similarities must not be over-interpreted and other substrates may be recognized in structurally similar MATE/DTXs, our analysis makes clear suggestions for potential substrates of white lupin MATE/DTX orthologs. These can be tested in future functional assays. Sequence comparisons and the high expression in mature clusters suggested *LaMATE* and *LaMATE3* as potential candidate genes for citrate efflux. *LaMATE* was specifically highly upregulated in mature clusters that massively efflux citrate, while immature, juvenile, and senescent cluster roots do not secrete large amounts of citrate (Neumann et al., 1999). Expression of *LaMATE3* was lower and was less cluster-stage-dependent, but expression was also highest in mature clusters; both transcripts were absent in leaves (Figure 2).

4.2 | Reverse genetics and electrophysiology fail to provide functional evidence for citrate transport by LaMATE and LaMATE3

LaMATE- and LaMATE3-expressing oocytes had significantly increased inward currents at very negative voltages compared to controls, especially at low external pH (Figure 3). Citrate preloading, however, did not much affect these currents. These currents were also not affected by replacing the choline cations by sodium (but by replacing

chloride). The reversal potentials were little affected by changes in the external pH and they were close to the reversal potential of chloride, suggesting that the ionic inward currents were mostly carried by chloride efflux. Somewhat unspecific, similar currents had been observed with the expression of various unrelated membrane proteins in the heterologous system oocytes (Tzounopoulos et al., 1995). Furthermore, similar currents were recorded after the expression of plant phosphate transporters, even in the absence of phosphate (Wang et al., 2014). We therefore consider it most likely that the elicited currents were from endogenous channels, unspecifically activated by LaMATE or LaMATE3 expression. If so, this would explain why no citrate (or genistein) transport was associated with their expression in oocytes. We note, however, that two vacuolar MATE/DTX homologs from Arabidopsis were suggested to function as chloride channels (Zhang et al., 2017). Indeed, we cannot rule out that the observed currents were directly carried by LaMATE and LaMATE3 proteins in oocytes. P-deficient white lupin roots contain anion channels in their plasma membranes (Zhang et al., 2004). As citrate is an anion and its release from oocytes might be stimulated by antiport with H^+, citrate efflux was expected to increase these inward currents, but also to shift the reversal potential toward more positive voltages. While currents were stimulated by low external pH, a substantial shift in the reversal potential was not observed, arguing against a major H^+/anion antiport mechanism in oocytes expressing LaMATEs. In agreement with these current recordings, oocytes injected with ^{13}C-labeled citrate, in which the efflux of ^{13}C label into the bath and the amount retained in the cells were measured, did also not support any major citrate efflux by LaMATEs in oocytes and no genistein transport (Figure 4, Figure S1). In these experiments, the estimated internal citrate concentration was in the range of ~3 mM, and this may be too low for substantial export. It is, however, highly unlikely that "poor" oocytes were responsible for the failure to directly record citrate currents/transport, as consistent results were obtained in six independent oocyte batches and large malate currents by LaALMT1 were successfully recorded from in part the same batches of oocytes (Zhou et al., 2020). Another heterologous expression system is thus required to understand LaMATEs function, as most likely both LaMATEs did not functionally express in oocytes (e.g. were not folded correctly in that heterologous host). It remains a question then, however, how injection of their mRNA evoked the observed citrate-independent inward currents.

We therefore targeted *LaMATE* via CRISPR/Cas9 in transgenic roots to obtain gene *knock-outs*. Genome editing was efficient and successful in composite hairy root transgenics of *L. albus*, but diverse mutations were obtained, as in the case of *LaALMT1* (Zhou et al., 2020). The transgenic roots must, however, probably be viewed as a mosaic or chimeric organ, containing (few) unmodified cells and different mutations within a single root (Zhou et al., 2020). With respect to the mutation types, different lengths of deletions and base changes/insertions were detected with the two different sgRNAs used (Figure 5), similar to findings in other plants (Puchta & Fauser, 2014; Zhang et al., 2016). CRISPR/Cas9 induced even a rather unusual 27 bp deletion in the root #4 genome, which occasionally results from the imperfect repair of double-strand breaks (Puchta & Fauser, 2014; Voytas, 2013). Considering the mutation types, we found combinations accounting for 60% among the tested plants (Figure 5), which is not uncommon (Zhang et al., 2014).

Compared to controls, only *matePS2*, but not *matePS1* mutants, had lower citrate (and malate) concentrations in exudates under P deficiency. However, the internal organic acid anion concentrations, both of citrate and of malate, tended to be decreased in parallel in the mutants (Figures 6 and 7). This suggests that lower malate in the tissue then resulted in less malate in the exudate and in the xylem sap. This possibly points to an indirect effect in the mutants on carboxylic acid metabolism, e.g. due to metabolic feedback regulation, which has been reported in other plant species, both for malate and citrate (Popova & Pinheiro de Carvalho, 1998; Wedding et al., 1990). With additional Al stress, both *matePS* mutants still released substantial citrate (Figure 6), but after the 2-day exposure to Al all plants appeared somewhat exhausted, as they did not have more citrate excretion than without addition of Al. Al is known to specifically boost citrate exudation in a different way than P-deficiency (Wang et al., 2007).

The explanatory power of these results from the plants with transgenic roots is clearly limited by the relatively large variance within sample groups. This has several reasons: First, the hairy root-transfected and regenerated plants were not as uniform as plants generated from seeds. Second, mutations in individual plants differed and thus not all mutations lead to full *knock-out* of LaMATE function. To overcome this latter limitation, we studied the exudation of citrate in composite transgenic mutants in which the *LaMATE* expression was suppressed by a *RNAi* construct (Figure 6). This *RNAi* construct efficiently repressed *LaMATE* expression (Uhde-Stone et al., 2005) and resulted in moderately reduced growth (−20%) of root-transgenic plants, but whether this impaired the secretion of citrate had not been studied (Uhde-Stone et al., 2005). Citrate secretion of *RNAi* plants did not differ from wild-type controls (Figure 6D), in agreement with the CRISPR transgenics, suggesting that hypothetical residual nonmutant root parts (Figure 5) unlikely explain the failure to suppress citrate exudation by CRISPR/Cas (Figure 6).

Potential off-targets of the *sgRNA matePS* constructs cannot be ruled out, although genome scanning did not identify a perfect off-target candidate match. The major organic acid in the xylem sap was malic acid, which was lowered by about 50%, consistent with reduced malate in the tissue (Figure 7). Related MATEs, such as AtFRD3, are responsible for assisting Fe translocation from the root to the shoot in Arabidopsis by transporting citrate (Durrett et al., 2007; Green & Rogers, 2004). LaMATE expression is strong in a rim around the root vasculature (Uhde-Stone et al., 2005), opening the possibility that LaMATE is also involved in metal-chelate root to shoot translocation in white lupin. The concentrations of shoot Fe and Zn were indeed slightly reduced in the *matePS2* mutant group, potentially a secondary effect of lower citrate and malate in the root or xylem (Figure 7). Metal concentration changes in the shoot thus may indirectly result from differences in the metal chelators available in the xylem sap.

The smaller biomass of composite plants in which *LaMATE* was silenced by *RNAi* (Uhde-Stone et al., 2005), may also result from

disturbed carboxylate flux and homeostasis, impaired metal allocation or other factors. In principle, it seems possible that another homolog of LaMATE, namely LaMATE3, might take over citrate efflux when LaMATE is missing, as it is the only member of the "citrate" branch of MATE/DTX transporters that is also expressed at high levels in mature clusters (Figures 1 and 2, Secco et al., 2014; Wang, Straub, et al., 2014). As LaMATE was (i) unable to complement the *frd3* phenotype in Arabidopsis (Uhde-Stone et al., 2005), (ii) citrate efflux remained in *RNAi* silenced roots, and (iii) citrate release remained high in both CRISPR mutant groups (*matePS1* and *matePS2*), we conclude that *LaMATE* has other functions than citrate exudation from mature cluster roots.

4.3 | Less genistein in *LaMATE*-mutant root exudates

In mature white lupin cluster roots, isoflavonoids and its glycosides are co-released with citrate under P-deficiency, shortly prior to the main peak of exudation, most likely to avoid rhizosphere microbiota consuming the released citrate. These compounds also have been implicated in the mobilization of P_i, but additionally decreased microbial growth and respiration, stimulated fungal sporulation, impaired citrate mineralization by rhizosphere microorganisms, and inhibited soil phosphohydrolase activities (Tomasi et al., 2008; Weisskopf, Tomasi, et al., 2006). Furthermore, iron deficiency induces the release of redox-active phenolics to mobilize iron (Rajniak et al., 2018) and the release of isoflavonoids may thus help to liberate P from Fe-P complexes. Interestingly, the release of the major isoflavonoid exuded by white lupin, genistein, was significantly suppressed by more than three-fold via targeting *LaMATE* in both mutant groups (Figure 8). This repression of genistein release was by far larger than the effect of the mutations on citrate or malate release and was consistently found in both mutant groups. Even if one argues that our failure to detect a strong reduction in citrate exudation in the mutants was due to insufficient *knock-out* or *knock-down* of *LaMATE* (by CRISPR or RNAi), one has to accept that the effect on genistein efflux was consistent and large (in contrast to the effect on citrate). This opens the possibility that LaMATE itself contributed to the export of this isoflavonoid, but we cannot rule out that this is again only a side effect of further unknown metabolic changes in the root tissue. If the substrate of LaMATE is indeed genistein, its inhibited export (in *mate* mutants) may have led to excessive genistein accumulation in the roots, which may not only be toxic to microbes, but also to the plant metabolism, especially when accumulated to high amounts as suspected to occur in root clusters under P deficiency. This ultimately may alter the entire metabolism; less carboxylate accumulation in the root tissue may be one consequence. Genistein may then indirectly impair the carboxylate metabolism (and lowered organic acid concentrations) of the roots in genome-edited plants and may also be responsible for the growth suppression of the *RNAi* plants (Uhde-Stone et al., 2005). Because we were not yet able to reconstitute functional genistein transport with LaMATE in a heterologous system such as oocytes (Figure S1), it is too early to conclude that LaMATE transported genistein directly.

However, we were surprised that our straightforward hypothesis based on homology considerations and numerous published reports—that LaMATE encodes the white lupin citrate transporter—was not supported by various independent experiments. It also remains puzzling that the MATE/DTX proteins from other species that transport various flavonoids or even flavonoid glycosides (Kitamura et al., 2016; Marinova et al., 2007; Takanashi et al., 2014; Zhao et al., 2011; Zhao & Dixon, 2009) clearly belong (by sequence) to another sub-branches of the MATE/DTX family (Figure 1). It remains a possibility that glycosides of genistein are transported by LaMATE outward across the cluster root membrane and that these are subsequently cleaved from its sugar via apoplastic enzymatic hydrolysis, a mechanism that is discussed for the isoflavonoid release in soybean (Sugiyama, 2019). This might also explain that that several other (unidentified) substances were altered in the exudate chromatograms (Figure 8). With several independent lines of evidence, we conclude that the function of LaMATE in white lupin clusters is, unexpectedly, not in citrate release. The model system white lupin apparently bears much interesting genetic secrets to be discovered, but our results also warrant a critical look on the function of MATE orthologs in other species.

ACKNOWLEDGMENTS

Yaping Zhou acknowledges the receipt of a studentship from the China Scholarship Council. The authors also acknowledge funds from the German Research Foundation (DFG) for work on cluster roots of white lupin to Uwe Ludewig The authors thank Dr. Benjamin Péret and Nicole Harzic for the lupin seeds, Dr. Jianbo Shen for the *Agrobacterium rhizogenes* strain A4T, Elke Dachtler, Helene Ochott and Deborah Schnell for laboratory help, Silvia Mancarella for the help with transformation, Dr. Holger Puchta for the CRISPR/Cas9 plasmids and the core facility of the University of Hohenheim for mass spectrometric analyses. Open access funding enabled and organized by Projekt DEAL.

AUTHOR CONTRIBUTIONS

Yaping Zhou performed most of the experiments and analyzed all data; Benjamin Neuhäuser, Philipp Olt helped with gene expression analysis and electrophysiology; Narges Moradtalab performed flavonoid HPLC measurements; William Bautista and Claudia Uhde-Stone participated in mutant generation and analysis; Günter Neumann participated in experimental design, analysis and writing; Yaping Zhou and Uwe Ludewig conceived the project, designed the experiments, and wrote the article with contributions of all the authors; Uwe Ludewig agrees to serve as the author responsible for contact and ensures communication.

DATA AVAILABILITY STATEMENT

Data will be made available on request from the corresponding author.

ORCID

Benjamin Neuhäuser https://orcid.org/0000-0002-2391-0598
Uwe Ludewig https://orcid.org/0000-0001-5456-1055

REFERENCES

Cheng, L., Bucciarelli, B., Shen, J., Allan, D. & Vance, C.P. (2011) Update on white lupin cluster root acclimation to phosphorus deficiency update on lupin cluster roots. *Plant Physiology*, 156, 1025–1032.

Development Core Team, R. (2008) *R: a language and environment for statistical computing*. Vienna, Austria: R Foundation for Statistical Computing.

Dinkelaker, B., Römheld, V. & Marschner, H. (1989) Citric acid excretion and precipitation of calcium citrate in the rhizosphere of white lupin (*Lupinus albus* L.). *Plant, Cell & Environment*, 1, 285–292.

Durrett, T.P., Gassmann, W. & Rogers, E.E. (2007) The FRD3-mediated efflux of citrate into the root vasculature is necessary for efficient iron translocation. *Plant Physiology*, 144, 197–205.

Edwards, K., Johnstone, C. & Thompson, C. (1991) A simple and rapid method for the preparation of plant genomic DNA for PCR analysis. *Nucl Acids Res*, 19, 1349.

Furukawa, J., Yamaji, N., Wang, H., Mitani, N., Murata, Y., Sato, K. et al. (2007) An aluminum-activated citrate transporter in barley. *Plant & Cell Physiology*, 48, 1081–1091.

Gardner, W., Barber, D. & Parbery, D. (1983) The acquisition of phosphorus by *Lupinus albus* L. *Plant and Soil*, 70, 107–124.

Gardner, W., Parbery, D. & Barber, D. (1981) Proteoid root morphology and function in *Lupinus albus*. *Plant and Soil*, 60, 143–147.

Green, L.S. & Rogers, E.E. (2004) FRD3 controls iron localization in *Arabidopsis*. *Plant Physiology*, 136, 2523–2531.

Haase, S., Neumann, G., Kania, A., Kuzyakov, Y., Römheld, V. & Kandeler, E. (2007) Atmospheric CO_2 and the N-nutritional status modifies nodulation, nodule-carbon supply and root exudation of *Phaseolus vulgaris* L. *Soil Biology and Biochemistry*, 39, 2208–2221.

Helliwell, C. & Waterhouse, P. (2003) Constructs and methods for high-throughput gene silencing in plants. *Methods*, 30, 289–295.

Hothorn, T., Bretz, F. & Westfall, P. (2008) Simultaneous inference in general parametric models. *Biometrical Journal*, 50, 346–363.

Hufnagel, B., Marques, A., Soriano, A., Marquès, L., Divol, F., Doumas, P. et al. (2020) High-quality genome sequence of white lupin provides insight into soil exploration and seed quality. *Nature Communications*, 11, 1–12.

Kitamura, S., Oono, Y. & Narumi, I. (2016) *Arabidopsis pab1*, a mutant with reduced anthocyanins in immature seeds from banyuls, harbors a mutation in the MATE transporter FFT. *Plant Molecular Biology*, 90, 7–18.

Lambers, H., Martinoia, E. & Renton, M. (2015) Plant adaptations to severely phosphorus-impoverished soils. *Current Opinion in Plant Biology*, 25, 23–31.

Li, Z., Liu, Z.-B., Xing, A., Moon, B.P., Koellhoffer, J.P., Huang, L. et al. (2015) Cas9-guide RNA directed genome editing in soybean. *Plant Physiology*, 169, 960–970.

Liu, J., Magalhaes, J.V., Shaff, J. & Kochian, L.V. (2009) Aluminum-activated citrate and malate transporters from the MATE and ALMT families function independently to confer *Arabidopsis* aluminum tolerance. *The Plant Journal*, 57, 389–399.

Ludewig, U., von Wirén, N. & Frommer, W.B. (2002) Uniport of NH4+ by the root hair plasma membrane ammonium transporter LeAMT1;1. *The Journal of Biological Chemistry*, 277, 13548–13555.

Magalhaes, J.V., Liu, J., Guimarães, C.T., Lana, U.G.P., Alves, V.M.C., Wang, Y.-H. et al. (2007) A gene in the multidrug and toxic compound extrusion (MATE) family confers aluminum tolerance in sorghum. *Nature Genetics*, 39, 1156–1161.

Marinova, K., Pourcel, L., Weder, B., Schwarz, M., Barron, D., Routaboul, J. M. et al. (2007) The Arabidopsis MATE transporter TT12 acts as a vacuolar flavonoid/H+-antiporter active in proanthocyanidin-accumulating cells of the seed coat. *plant Cell*, 19, 2023–2038.

Mayer, M. & Ludewig, U. (2006) Role of AMT1;1 in NH4+ acquisition in *Arabidopsis thaliana*. *Plant Biology*, 8, 522–528.

Mikami, M., Toki, S. & Endo, M. (2015) Comparison of CRISPR/Cas9 expression constructs for efficient targeted mutagenesis in rice. *Plant Molecular Biology*, 88, 561–572.

Miyauchi, H., Moriyama, S., Kusakizako, T., Kumazaki, K., Nakane, T., Yamashita, K. et al. (2017) Structural basis for xenobiotic extrusion by eukaryotic MATE transporter. *Nature Communications*, 8, 1–11.

Neumann, G. & Martinoia, E. (2002) Cluster roots – an underground adaptation for survival in extreme environments. *Trends in Plant Science*, 7, 162–167.

Neumann, G., Massonneau, A., Martinoia, E. & Römheld, V. (1999) Physiological adaptations to phosphorus deficiency during proteoid root development in white lupin. *Planta*, 208, 373–382.

Neumann, G. & Römheld, V. (1999) Root excretion of carboxylic acids and protons in phosphorus-deficient plants. *Plant and Soil*, 211, 121–130.

Neumann, G. & Römheld, V. (2007) The release of root exudates as affected by the plant physiological status. In: Pinto, R., Varanini, Z. & Nannipieri, Z. (Eds.) *The rhizosphere: biochemistry and organic substances at the soil–plant interface*, 2nd edition. Boca Raton, FL: CRC Press.

O'Rourke, J.A., Yang, S.S., Miller, S.S., Bucciarelli, B., Liu, J., Rydeen, A. et al. (2013) An RNA-Seq transcriptome analysis of orthophosphate-deficient white lupin reveals novel insights into phosphorus acclimation in plants. *Plant Physiology*, 161, 705–724.

Popova, T.N. & Pinheiro de Carvalho, M.A.A. (1998) Citrate and isocitrate in plant metabolism. *Biochimica et Biophysica Acta*, 1364, 307–325.

Puchta, H. & Fauser, F. (2014) Synthetic nucleases for genome engineering in plants: prospects for a bright future. *The Plant Journal*, 78, 727–741.

Purnell, H.M. (1960) Studies of the family Proteaceae. I. Anatomy and morphology of the roots of some Victorian species. *Australian Journal of Botany*, 8, 38–50.

Quandt, H.J., Pühler, A. & Broer, I. (1993) Transgenic root nodules of *Vicia hirsuta*: a fast and efficient system for the study of gene expression in indeterminate-type nodules. *Molecular Plant-Microbe Interactions*, 6, 699–706.

Raghothama, K.G. (1999) Phosphate acquisition. *Annual Review of Plant Physiology and Plant Molecular Biology*, 50, 665–693.

Rajniak, J., Giehl, R.F., Chang, E., Murgia, I., von Wirén, N. & Sattely, E.S. (2018) Biosynthesis of redox-active metabolites in response to iron deficiency in plants. *Nature Chemical Biology*, 14, 442–450.

Schiml, S., Fauser, F. & Puchta, H. (2016) CRISPR/Cas-mediated site-specific mutagenesis in *Arabidopsis thaliana* using Cas9 nucleases and paired nickases. In: *Chromosome and genomic engineering in plants*. New York, NY: Humana Press, pp. 111–122.

Secco, D., Shou, H., Whelan, J. & Berkowitz, O. (2014) RNA-seq analysis identifies an intricate regulatory network controlling cluster root development in white lupin. *BMC Genomics*, 15, 230.

Serrano, M., Wang, B., Aryal, B., Garcion, C., Abou-Mansour, E., Heck, S. et al. (2013) Export of salicylic acid from the chloroplast requires the MATE-like transporter EDS5. *Plant Physiology*, 162, 1815–1821.

Sugiyama, A. (2019) The soybean rhizosphere: metabolites, microbes, and beyond - a review. *Journal of Advanced Research*, 19, 67–73.

Takanashi, K., Shitan, N. & Yazaki, K. (2014) The multidrug and toxic compound extrusion (MATE) family in plants. *Plant Biotechnology*, 31, 417–430.

Tomasi, N., Weisskopf, L., Renella, G., Landi, L., Pinton, R., Varanini, Z. et al. (2008) Flavonoids of white lupin roots participate in phosphorus mobilization from soil. *Soil Biology and Biochemistry*, 40, 1971–1974.

Tzounopoulos, T., Maylie, J. & Adelman, J.P. (1995) Induction of endogenous channels by high levels of heterologous membrane proteins in *Xenopus* oocytes. *Biophysical Journal*, 69, 904–908.

Uhde-Stone, C., Liu, J., Zinn, K.E., Allan, D.L. & Vance, C.P. (2005) Transgenic proteoid roots of white lupin: a vehicle for characterizing and silencing root genes involved in adaptation to P stress. *The Plant Journal*, 44, 840–853.

Upadhyay, N., Kar, D., Deepak Mahajan, B., Nanda, S., Rahiman, R., Panchakshari, N. et al. (2019) The multitasking abilities of MATE transporters in plants. *Journal of Experimental Botany*, 70, 4643–4656.

Vance, C.P., Uhde-Stone, C. & Allan, D.L. (2003) Phosphorus acquisition and use: critical adaptations by plants for securing a nonrenewable resource. *New Phytologist*, 157, 423–447.

Voytas, D.F. (2013) Plant genome engineering with sequence-specific nucleases. *Annual Review of Plant Biology*, 64, 327–350.

Wang, B.L., Shen, J.B., Zhang, W.H., Zhang, F.S. & Neumann, G. (2007) Citrate exudation from white lupin induced by phosphorus deficiency differs from that induced by aluminum. *New Phytologist*, 176, 581–589.

Wang, X., Wang, Y., Piñeros, M.A., Wang, Z., Wang, W., Li, C. et al. (2014) Phosphate transporters OsPHT1;9 and OsPHT1;10 are involved in phosphate uptake in rice. *Plant, Cell & Environment*, 37, 1159–1170.

Wang, Y. & Lambers, H. (2020) Root-released organic anions in response to low phosphorus availability: recent progress, challenges and future perspectives. *Plant and Soil*, 447, 135–156.

Wang, Z., Straub, D., Yang, H., Kania, A., Shen, J., Ludewig, U. et al. (2014) The regulatory network of cluster-root function and development in phosphate-deficient white lupin (*Lupinus albus*) identified by transcriptome sequencing. *Physiologia Plantarum*, 151, 323–338.

Wasaki, J., Omura, M., Ando, M., Shinano, T., Osaki, M. & Tadano, T. (1999) Secreting portion of acid phosphatase in roots of lupin (*Lupinus albus* L.) and a key signal for the secretion from the roots. *Soil Science & Plant Nutrition*, 45, 937–945.

Watt, M. & Evans, J.R. (1999) Proteoid roots. Physiology and development. *Plant Physiology*, 121, 317–323.

Wedding, R.T., Kay Black, M. & Meyer, C.R. (1990) Inhibition of phosphoenolpyruvate carboxylase by malate. *Plant Physiology*, 92, 456–461.

Weisskopf, L., Abou-Mansour, E., Fromin, N., Tomasi, N., Santelia, D., Edelkott, I. et al. (2006) White lupin has developed a complex strategy to limit microbial degradation of secreted citrate required for phosphate acquisition. *Plant, Cell & Environment*, 29, 919–927.

Weisskopf, L., Fromin, N., Tomasi, N., Aragno, M. & Martinoia, E. (2005) Secretion activity of white lupin's cluster roots influences bacterial abundance, function and community structure. *Plant and Soil*, 268, 181–194.

Weisskopf, L., Tomasi, N., Santelia, D., Martinoia, E., Langlade, N.B., Tabacchi, R. et al. (2006) Isoflavonoid exudation from white lupin roots is influenced by phosphate supply, root type and cluster-root stage. *The New Phytologist*, 171, 657–668.

Xu, W.F., Zhang, Q., Yuan, W., Xu, F.Y., Aslam, M.M., Miao, R. et al. (2020) The genome evolution and low-phosphorus adaptation in white lupin. *Nature Communications*, 11, 1–13.

Yokosho, K., Yamaji, N., Ueno, D., Mitani, N. & Ma, J.F. (2009) OsFRDL1 is a citrate transporter required for efficient translocation of iron in rice. *Plant Physiology*, 149, 297–305.

Zhang, B., Yang, X., Yang, C., Li, M. & Guo, Y. (2016) Exploiting the CRISPR/Cas9 system for targeted genome mutagenesis in petunia. *Scientific Reports*, 6, 20315.

Zhang, H., Zhang, J., Wei, P., Zhang, B., Gou, F., Feng, Z. et al. (2014) The CRISPR/Cas9 system produces specific and homozygous targeted gene editing in rice in one generation. *Plant Biotechnology Journal*, 12, 797–807.

Zhang, H., Zhu, H., Pan, Y., Yu, Y., Luan, S. & Li, L. (2014) A DTX/MATE-type transporter facilitates abscisic acid efflux and modulates ABA sensitivity and drought tolerance in *Arabidopsis*. *Molecular Plant*, 7, 1522–1532.

Zhang, W.H., Ryan, P.R. & Tyerman, S.D. (2004) Citrate-permeable channels in the plasma membrane of cluster roots from white lupin. *Plant Physiology*, 136, 3771–3783.

Zhang, W.H., Zhao, F.G., Tang, R.J., Yu, X.Y., Song, J.L., Wang, Y. et al. (2017) Two tonoplast MATE proteins function as turgor-regulating chloride channels in *Arabidopsis*. *Proceedings of the National Academy of Sciences of the United States of America*, 114, E2036–E2045.

Zhao, J. & Dixon, R.A. (2009) MATE transporters facilitate vacuolar uptake of epicatechin 3′-O-Glucoside for proanthocyanidin biosynthesis in *Medicago truncatula* and *Arabidopsis*. *plant Cell*, 21, 2323–2340.

Zhao, J., Huhman, D., Shadle, G., He, X.Z., Sumner, L.W., Tang, Y. et al. (2011) MATE2 mediates vacuolar sequestration of flavonoid glycosides and glycoside malonates in *Medicago truncatula*. *plant Cell*, 23, 1536–1555.

Zhou, Y., Neuhäuser, B., Neumann, G. & Ludewig, U. (2020) LaALMT1 mediates malate release from phosphorus-deficient white lupin root tips and metal root to shoot translocation. *Plant, Cell & Environment*, 47, 1691–1706.

Zhou, Y., Sarker, U., Neumann, G. & Ludewig, U. (2019) The LaCEP1 peptide modulates cluster root morphology in *Lupinus albus*. *Physiologia Plantarum*, 166, 525–537.

SUPPORTING INFORMATION

Additional supporting information may be found online in the Supporting Information section at the end of this article.

How to cite this article: Zhou, Y., Olt, P., Neuhäuser, B., Moradtalab, N., Bautista, W., Uhde-Stone, C. et al. (2021) Loss of LaMATE impairs isoflavonoid release from cluster roots of phosphorus-deficient white lupin. *Physiologia Plantarum*, 173 (3), 1207–1220. Available from: https://doi.org/10.1111/ppl.13515